


# Induction of Chondrogenic Differentiation in Human Mesenchymal Stem Cells Cultured on Human Demineralized Bone Matrix Scaffold under Hydrostatic Pressure

Saeid Reza Shahmoradi<sup>1</sup> · Maryam Kabir Salmani<sup>1</sup> · Hamid Reza Soleimanpour<sup>1</sup> · Amir Hossein Tavakoli<sup>2</sup> · Kazem Hosaini<sup>2</sup> · Nooshin Haghighipour<sup>3</sup> · Shahin Bonakdar<sup>3</sup> 

Received: 16 June 2018 / Revised: 24 September 2018 / Accepted: 1 October 2018 / Published online: 17 November 2018  
© The Korean Tissue Engineering and Regenerative Medicine Society and Springer Science+Business Media B.V., part of Springer Nature 2018

## Abstract

**BACKGROUND:** Articular cartilage damage is still a troublesome problem. Hence, several researches have been performed for cartilage repair. The aim of this study was to evaluate the chondrogenicity of demineralized bone matrix (DBM) scaffolds under cyclic hydrostatic pressure (CHP) *in vitro*.

**METHODS:** In this study, CHP was applied to human bone marrow mesenchymal stem cells (hBMSCs) seeded on DBM scaffolds at a pressure of 5 MPa with a frequency of 0.5 Hz and 4 h per day for 1 week. Changes in chondrogenic and osteogenic gene expressions were analyzed by quantifying mRNA signal level of Sox9, collagen type I, collagen type II, aggrecan (ACAN), Osteocalcin, and Runx2. Histological analysis was carried out by hematoxylin and eosin, and Alcian blue staining. Moreover, DMMB and immunofluorescence staining were used for glycosaminoglycan (GAG) and collagen type II detection, respectively.

**RESULTS:** Real-time PCR demonstrated that applying CHP to hBMSCs in DBM scaffolds increased mRNA levels by 1.3-fold, 1.2-fold, and 1.7-fold ( $p < 0.005$ ) for Sox9, Col2, and ACAN, respectively by day 21, whereas it decreased mRNA levels by 0.7-fold and 0.8-fold ( $p < 0.05$ ) for Runx2 and osteocalcin, respectively. Additionally, in the presence of TGF- $\beta$ 1 growth factor (10 ng/ml), CHP further increased mRNA levels for the mentioned genes (Sox9, Col2, and ACAN) by 1.4-fold, 1.3-fold and 2.5-fold ( $p < 0.005$ ), respectively. Furthermore, in histological assessment, it was observed that the extracellular matrix contained GAG and type II collagen in scaffolds under CHP and CHP with TGF- $\beta$ 1, respectively.

**CONCLUSION:** The osteo-inductive DBM scaffolds showed chondrogenic characteristics under hydrostatic pressure. Our study can be a fundamental study for the use of DBM in articular cartilage defects *in vivo* and lead to production of novel scaffolds with two different characteristics to regenerate both bone and cartilage simultaneously.

✉ Maryam Kabir Salmani  
maryam@nigeb.ac.ir

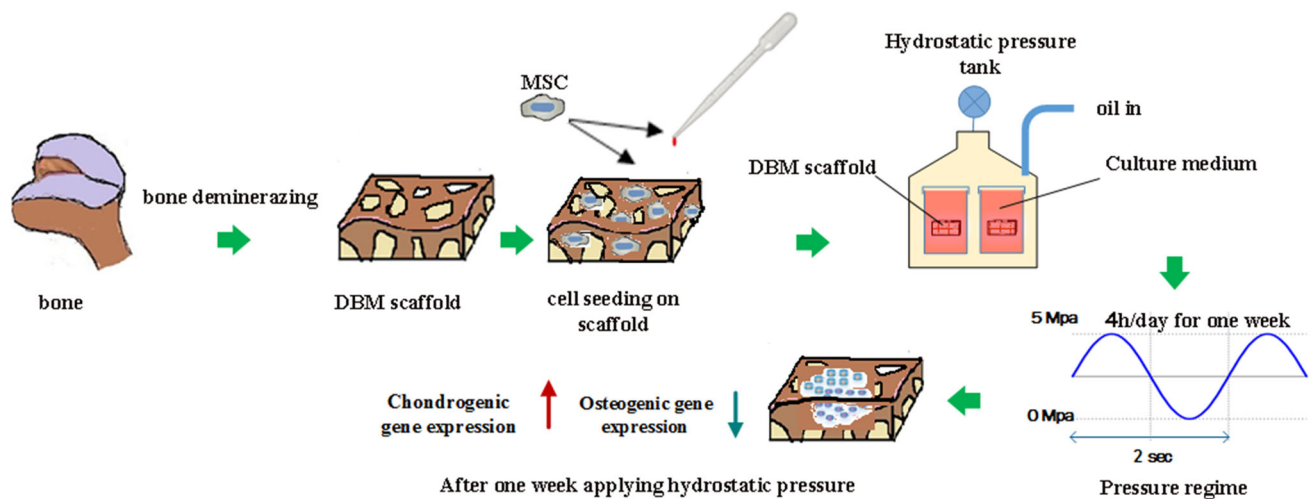
✉ Shahin Bonakdar  
sh\_bonakdar@pasteur.ac.ir

<sup>1</sup> Biomaterials and Tissue Engineering Department, Stem Cell Division, National Institute of Genetic Engineering and Biotechnology, Shahrak-e Pajooesh, km 15, Tehran - Karaj Highway, Tehran 1497716316, Iran

<sup>2</sup> Iranian Tissue Bank, Imam khomani Hospital, University of Medical Sciences, Keshavarz Blvd, Tehran 1419733141, Iran

<sup>3</sup> National Cell Bank Department, Pasteur Institute of Iran (IPI), No. 69, Pasteur Ave, Tehran 1316943551, Iran

## Graphical abstract



**Keywords** Bone marrow mesenchymal stem cells · Chondrogenic differentiation · Hydrostatic pressure · Demineralized bone matrix scaffold

## 1 Introduction

Articular cartilage has poor ability for self-repair due to low cell density (particularly in adults), lack of nerves, and being largely avascular [1, 2]. A number of surgical techniques (such as autografting) can be helpful to regenerate cartilaginous defects; however, there are often limitations for their application. Instead of normal cartilage tissue, fibrocartilage tissue is created after most surgical procedures [3]. Therefore, tissue engineering using new scaffolds is an alternative for developing cartilaginous grafts as well as a promising approach for regenerating normal cartilage [4–6]. It has been shown that microenvironment affects cell differentiation, so the generation of synthetic scaffolds is being developed from natural ECM. To mimic natural properties, a number of biomaterials such as collagen, chitosan, silk, poly (vinyl alcohol) (PVA), polyurethane (PU), polycaprolacton (PCL), poly lactic-acid, and hydrogel as well as their composites have been used as artificial scaffolds. However, there has been increasing interest in seeding mesenchymal stem cells (MSCs) onto scaffolds and hydrogels [7–14].

It is known that demineralized bone matrix (DBM) scaffolds have osteo-inductive and osteo-conductive properties. They are most frequently used to accomplish bone fusion or replacement procedures and restore the bone lost during injury and are a promising therapeutic option for skeletal defects [15–17]. Spongy structure and flexibility (in hydrated state) are important properties of DBM scaffolds, which are composed of collagen (mostly type I and a few type IV and X), non-collagenous proteins, and growth

factors, as well as variable percentages of calcium phosphate [18].

Mechanical signals play a critical role in regulating the behavior of MSCs [19–21]. It has been shown that dynamic compression inhibits chondrogenesis if used at the beginning of growth factor induced differentiation [22, 23]. Functional properties of cartilaginous tissue can be increased by applying dynamic compression on bone marrow derived MSCs only after the initiation of chondrogenesis [24]. Some studies demonstrated that applying cyclic hydrostatic pressure on mesenchymal stem cells within the physiological range of 1–18 MPa can lead to an increase in mRNA expression of collagen type II, aggrecan, and proteoglycan [25–30]. Furthermore, it has been shown that applying CHP to hASCs in three dimensional (3D) cultures enhances chondrogenic gene markers without the application of growth factors [31].

As previously indicated, over the past few decades, various scaffolds and effect of mechanical signals have been studied for application in cartilage tissue regeneration. Therefore we were looking for a scaffold with a structure close to real condition which can well transfer the mechanical force to cells. Moreover, this study was conducted using human bone marrow mesenchymal stem cells (hBMSCs), since they have been reported to possess higher chondrogenic potential than human adipose stem cells (hASCs) under similar conditions [32–34]. Consequently, DBM scaffolds were selected, due to their natural base and being more flexible in the hydrated state. Since articular cartilage cells are under hydrostatic pressure, and the cartilage and bone tissues are firmly attached, simultaneous

bone and cartilage differentiation is crucial in this study. We hypothesized that combination of DBM scaffold, hBMSCs and hydrostatic pressure can mimic the natural microenvironment thus enabling simultaneous chondrogenic and osteogenic differentiation. On the other hand, these bone-like scaffolds are inherently osteo-inductive with chondrogenic properties. Furthermore, this research can be an introduction to development of new scaffolds supporting the bone from one side and helping to cartilage regeneration from the other side.

## 2 Materials and methods

### 2.1 Preparation of DBM scaffolds

In this study, the bone chips were prepared in the Iranian Tissue Engineering and Regenerative Medicine Center (ITERM) at Imam Khomeini Hospital according to the following procedure. The head of femur and cartilage tissue were used in order to produce a compact scaffold with fine pores. We cut two femur bone samples with  $6 \times 25 \times 25 \text{ mm}^3$  dimensions using a chain saw under strictly sterile conditions. The prepared samples were sequentially washed in different solutions, including distilled water, ethyl ether (to remove fat and blood from bone tissues for 4 h), and 5% ethanol-hydrochloric acid (to remove minerals). Each step took 45 min to be accomplished. The final samples were rinsed in PBS until their pH reached 7–7.4 and were then freeze-dried and sterilized by gamma radiation.

### 2.2 Porosity measurement

The pores size and their distribution, in scaffolds were measured using a mercury porosimeter (PASCAL 140 Thermo Finning, Rodano, Italy). To measure porosity, the samples ( $n = 3$ ) with nearly  $5 \times 5 \times 5 \text{ mm}^3$  dimensions were utilized. The shape of porosities was readily observable by an optical (Olympus cx23) and scanning electron microscope (AIS2100C, SERON TECHNOLOGIES, Uiwang, South Korea).

### 2.3 Compressive and tensile strength analysis

The compressive strength of samples was measured using universal strength testing machine (STM-20 Santam Co; Iran). Three samples with a dimension of  $5 \times 5 \times 6 \text{ mm}^3$  were tested at compression rate of 10 mm/min using a 20 KN load cell. The tensile strength was also measured with universal strength testing machine (STM-20). The samples with a dimension of  $5 \times 5 \times 20 \text{ mm}^3$  were tightened lengthwise between tensile fixtures. The tests were

performed in triplicate under the tensile stretch rate of 5 mm/min until the samples disintegrated.

### 2.4 Viability analysis

The extractions were obtained according to provisions of ISO 10993-12 standard, where 1 ml of Dulbecco's Modified Eagle's Medium (DMEM) was added to a 0.2 g sample and the container was stored in an incubator containing 5% CO<sub>2</sub> for 7 and 21 days at 37 °C. An equal volume of the culture medium was stored in the same conditions as negative control, and sodium lauryl sulfate (Merck) was considered as positive control. Cell viability was studied using 3-(4,5-dimethyl-2-thiazolyl)-2,5-diphenyltetrazolium bromide (MTT). Briefly,  $1 \times 10^4$  cells were seeded in a 96-well culture plate and incubated at 37 °C. After 24 h, the culture medium of each well was removed; the extracts were added to the wells and incubated for 24 h. Then, the medium was eliminated, and 100 µl MTT (with 0.5 mg/ml concentration) was added to each well. After 4 h, the solution was replaced with 100 µl isopropanol to solve the purple crystals. The concentration of the solved materials was measured by an ELISA reader (Epoch 2, BioTek, Bad Friedrichshall, Germany) at 545 nm wavelength, and viability (%) was calculated from Eq. (1):

$$\text{Viability}\% = (\text{ODs}/\text{ODc}) \times 100 \quad (1)$$

where ODs is average optical density of the sample and OD<sub>C</sub> is the average optical density of negative control.

### 2.5 Scanning electron microscopy

After 48 h of cell seeding on DBM, to visualize cell attachment and microstructure of samples, the scaffolds were fixed by 4% glutaraldehyde (Sigma, Cleveland, OH, USA), dehydrated through ethanol series and then observed by scanning electron microscope.

### 2.6 Degradation

In order to study the degradability properties, water absorption of the scaffolds was investigated as a function of weight changes of the scaffolds, which were immersed in deionized water at 37 °C. It was predicted that the scaffold should witness an increase in weight due to the absorbed water, followed by a downward trend of weight loss due to degradation. In this examination, samples ( $n = 3$ ) were firstly weighed in a dry state using a scale with 0.1 mg accuracy. They were then incubated in deionized water at 37 °C. Finally, the samples were removed and weighed at consecutive intervals after the

initial conditions. The percentage of water uptake can be determined from the following Eq. (2):

$$\text{The percentage of water uptake} = [(W_W - W_D)/W_D] * 100 \quad (2)$$

where  $W_W$  is, in fact, the weight of scaffold in the hydrated state and  $W_D$  is the weight of scaffold in the dry state [10].

## 2.7 Cell seeding experiment

Human bone marrow mesenchymal stem cells were purchased from Royan Institute (Tehran, Iran). As specified by Royan Institute, hBMSCs are harvested from normal bone marrows. These cells are positive for CD105, CD166, CD44, and CD29 but are negative for CD14, CD34, and CD45. hBMSCs were cultured in DMEM/Ham's-F12 (Gibco, Pittsburgh, PA, USA) with penicillin (100 U/ml), Streptomycin (100 µg/ml), and FBS 10% (Gibco, Pittsburgh, PA, USA). The scaffolds were initially washed with PBS; 1 ml of culture medium was added to each sample, which were stored to be absorbed into the scaffold. A number of  $2 \times 10^5$  cell/cm<sup>3</sup> in 100 µl was seeded on each scaffold and transferred to incubator for 3 h. Afterwards, the culture medium was added to each scaffold.

## 3 3D culture under hydrostatic pressure

Four different groups were considered to study the chondrogenic differentiation, which are summarized in Table 1. The first group was placed under hydrostatic pressure in culture medium (DMEM/Ham's-F12) and was named CHP. The second group was preserved under hydrostatic pressure in chondrogenic medium (DMEM/Ham's-F12 + TGFβ1) and was named (CHP + TGF). The third group was placed in chondrogenic culture medium without loading (S + TGF). Finally, the stem cells cultured on DBM scaffold in DMEM/Ham's-F12 medium were considered as the fourth group (S or con). All the groups were assayed on the 21st day. After 14 days, the first and second groups were subjected to hydrostatic loading for 7 days

under 5 MPa pressure and 0.5 Hz frequency for a 4 h per day regime, which is schematically depicted in Fig. 1. The expression of five genes, including Col1, Col2, aggrecan (ACAN), GAPDH, and Sox9 was evaluated at the end of the 2nd and 3rd weeks. Furthermore, given the bony nature of scaffolds and the previous reports suggesting osteo-inductive and osteo-conductive properties of allograft scaffolds, the expression of osteocalcin and Runx2 was also assessed. In addition, DMMB method was used for assessing the expression of glycosaminoglycan (GAG) protein. Histology and immunofluorescence staining were used for the evaluation of extracellular matrix.

## 3.1 Histological and immunofluorescence analysis

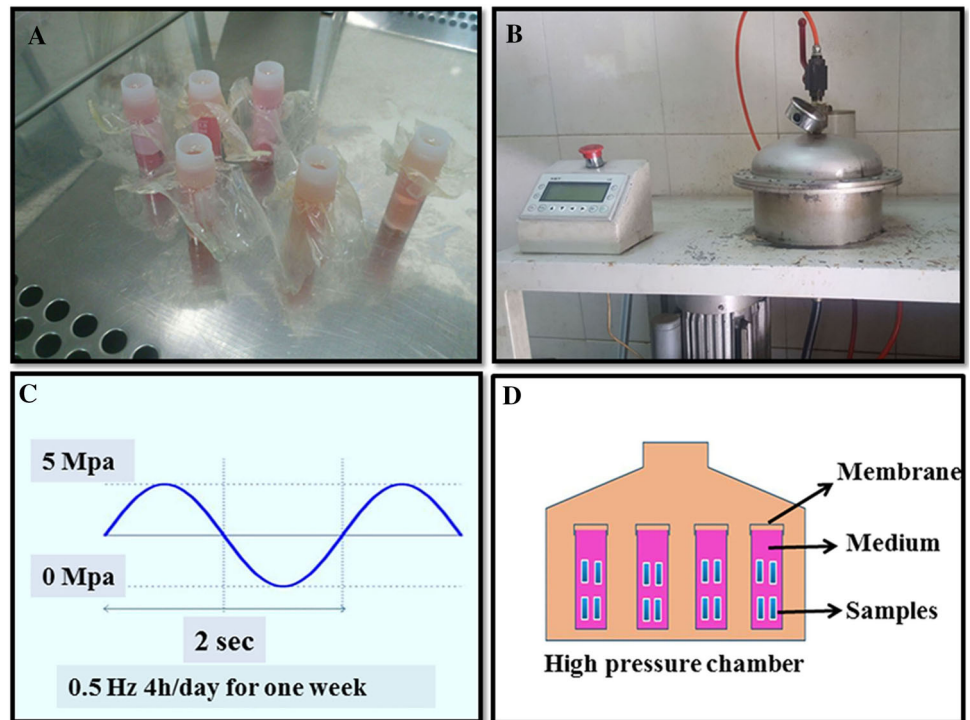
At the end of the third week, the samples were fixed in 10% formalin, dehydrated, and embedded into paraffin blocks that were cut into 6 µm sections. Afterwards, the sections were deparaffinized with xylene and rehydrated with alcohol to PBS series. The sections were then analyzed by light microscopy using standard hematoxylin and eosin staining to determine cell morphology in each group (Olympus ix53, Tokyo, Japan). Moreover, Alcian blue was used for GAG identification in the matrix. Finally, immunohistochemistry was carried out according to the following procedure. After fixation in formalin, the samples were washed with PBS for 15 min and then placed in Triton X100 for 10 min to permeabilize the cell membrane. Afterwards, the samples were three times washed with PBS and treated with BSA for 30 min in a humidified chamber at room temperature. The samples were again washed with PBS, and finally, 50 µl primary antibody (Novus Mouse monoclonal antibody anti collagen type II) was added. After 1 h, the samples were three times washed with PBS, each time for 5 min. In the next step, the secondary antibody (polyclonal antibody anti mouse IgG) was added to the samples in similar conditions to the primary one but in darkness, and the samples were maintained for 1 h. Subsequently, the samples were carefully washed three times with PBS and stained with Hoechst 33342 (Sigma, Cleveland, OH, USA) to detect cell nuclei. The constructs

**Table 1** Characteristics of the groups used in the assessment

Group	Scaffold	Task	TGF	CHP	Weeks
S	3D-DBM	Control	–	–	W1–W3
S + TGF	3D-DBM	Static sample	✓	–	W1–W3
CHP + TGF	3D-DBM	Cyclic Hydrostatic presser Sample	✓	✓	W3
CHP			–	✓	

S: Samples in “static culture” condition; S+TGF: Samples in “static culture with chondrogenic medium” condition; CHP: Samples in “Cyclic hydrostatic pressure” condition; CHP+TGF: Samples in “Cyclic hydrostatic pressure with chondrogenic medium” condition

**Fig. 1** Hydrostatic pressure system. **A** Isolated tubes containing samples. **B** Hydrostatic pressure machine. **C** The regime of cyclic hydrostatic pressure applied to samples. **D** Schematic of hydrostatic pressure chamber with samples



were viewed at room temperature with a fluorescence microscope (Leica DMi8, Wetzlar, Germany).

### 3.2 Real-time PCR

The samples from each group were analyzed on days 14 and 21 for quantitative reverse transcriptase polymerase chain reaction (qRT-PCR) analysis in which Thermo Cycler device and Master Mix kit (ABI, Carlsbad, CA, USA) were used. To ensure accuracy, three samples were taken from each group per each gene. Given the nature of the scaffolds used in this project and for the purpose of assessment, the effect of hydrostatic pressure on the mentioned scaffolds, as well as osteocalcin and Runx2 genes expressed in osteogenesis were assessed in addition to Col1, Col2, ACAN, Sox9, and GAPDH.

### 3.3 Determination of glycosaminoglycan (GAG) by DMMB staining

The glycosaminoglycan content was determined by the quantity quantification of sulfated GAGs released into media using 1,9-dimethylmethylene blue (DMMB; Sigma, Cleveland, OH, USA) staining method at pH = 6.8. After 7, 14, and 21 days of cell seeding, 500  $\mu$ l medium from each group was aspirated and transferred to a 2 ml tube. Then, 1.5 ml acetone (Merck, Kenilworth, NJ, USA) was added and kept at  $-20^{\circ}\text{C}$  for 24 h. Then, the samples were centrifuged at 1800 rpm for 30 min at  $-4^{\circ}\text{C}$ . The

sediment was suspended in 100  $\mu$ l PBS containing 20  $\mu$ g/ml papain and activated with 5 mM cysteine; subsequently, the samples were incubated at  $60^{\circ}\text{C}$  for 16 h and were boiled for 15 min. A known concentration of chondroitin sulfate (Sigma) was used as working range of the standard solution. The GAG content was quantified with an ELISA reader (Epoch 2, BioTek, Bad Friedrichshall, Germany) at 545 nm.

### 3.4 Statistical analysis

One-way analysis of variance (ANOVA) was used for all quantitative data reported in this paper. The results were considered significant with  $p < 0.05$ . Each experimental group was evaluated on at least three samples ( $n = 3$ ).

## 4 Results

### 4.1 Porosity

The pore size has an important role in nutrient transfer, cell attachment, and ingrowth. Interconnected pores with larger sizes can easily transport materials, nutrients, and metabolic waste. However, small pores in scaffold can lead to stronger cell attachment but have poor ability to transport gas, nutrient, and metabolic waste [35]. In this study, the samples pore sizes were assessed in an anisotropic range of interconnected pores. Small pores with an approximate size

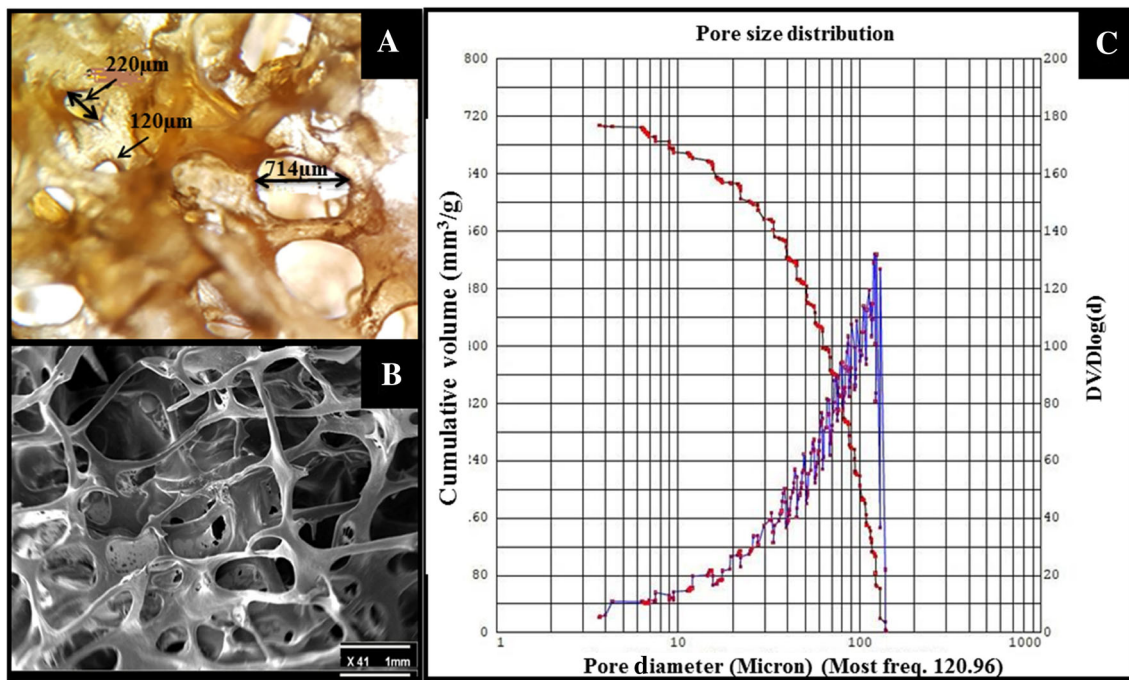


**Fig. 2** Scaffold porosity assay. **A** Optical microscope image of scaffolds, which shows the shape and size of porosity with  $\times 40$  magnification. **B** SEM image showing contraction of the scaffold

of  $5 \pm 2.02 \mu\text{m}$  and large ones with  $720 \pm 30.50 \mu\text{m}$  dimensions were detected. The most frequent size was seen in  $120 \pm 5.00 \mu\text{m}$  using a mercury porosimeter. This variation is affected by the type of bone and age of the donor. Figure 2 depicts porosities and their distribution.

The size and shape of porosities in the scaffolds were assessed by an optical microscope. It was found that the porosities were spherical-oval in shape. Moreover, the pores were open and located in an interconnected network.

#### 4.2 Compressive and tensile strength

Results obtained from this experiment showed that in the hydrated state, the scaffolds can be compressed to approximately  $57 \pm 5\%$  of their initial length (Fig. 3), which changes their elastic form and affects the transfer of hydrostatic pressure to the attached cells in the scaffold, finally influencing cell signaling and differentiation.

#### 4.3 Cell viability assessment

The results showed that compared to the negative control group, the viability of cells in contact with the scaffolds were  $88 \pm 2.5\%$  and  $80 \pm 0.2.6\%$  during 7 and 21 days, respectively, suggesting the non-cytotoxicity of the extract isolated from the samples and the significance ( $p < 0.05$ ) of viability in both samples compared to control (Fig. 4).

with  $\times 41$  magnification. **C** Mercury porosimeter analysis, the blue line shows pore size distribution and the red line is cumulative volume of pores in the scaffolds

#### 4.4 Electron scanning microscopy

Figure 5 shows electron scanning microscopic (SEM) image 48 h after cell culture, which determines the cells attached to the surface and overspread on it.

#### 4.5 Degradation of scaffolds

Based on the results, it turns out that the above-mentioned scaffolds began to degrade after the third week with a slow degradability slope. Figure 6 shows that water uptake increases until 24 h, then remains constant, and decreases after 48 h due to scaffold degradation. However, after 3 weeks, the changes (degradation) become significant ( $p < 0.05$ ).

#### 4.6 Histological and immunofluorescence analysis

H&E staining showed that the cells were distributed throughout the constructs of all groups; however, in Fig. 6A, CHP and CHP + TGF groups were denser and indicated the homogenous distribution of cells within the matrix, as compared to the other groups. Moreover, the shape of cells was spherical to spindle-like in S + TGF, CHP, and CHP + TGF groups, whereas it was spindle-like in the control group (S). Alcian blue staining (Fig. 6B) showed a positive reaction in CHP and CHP + TGF groups, and there was a slightly higher intensity of staining

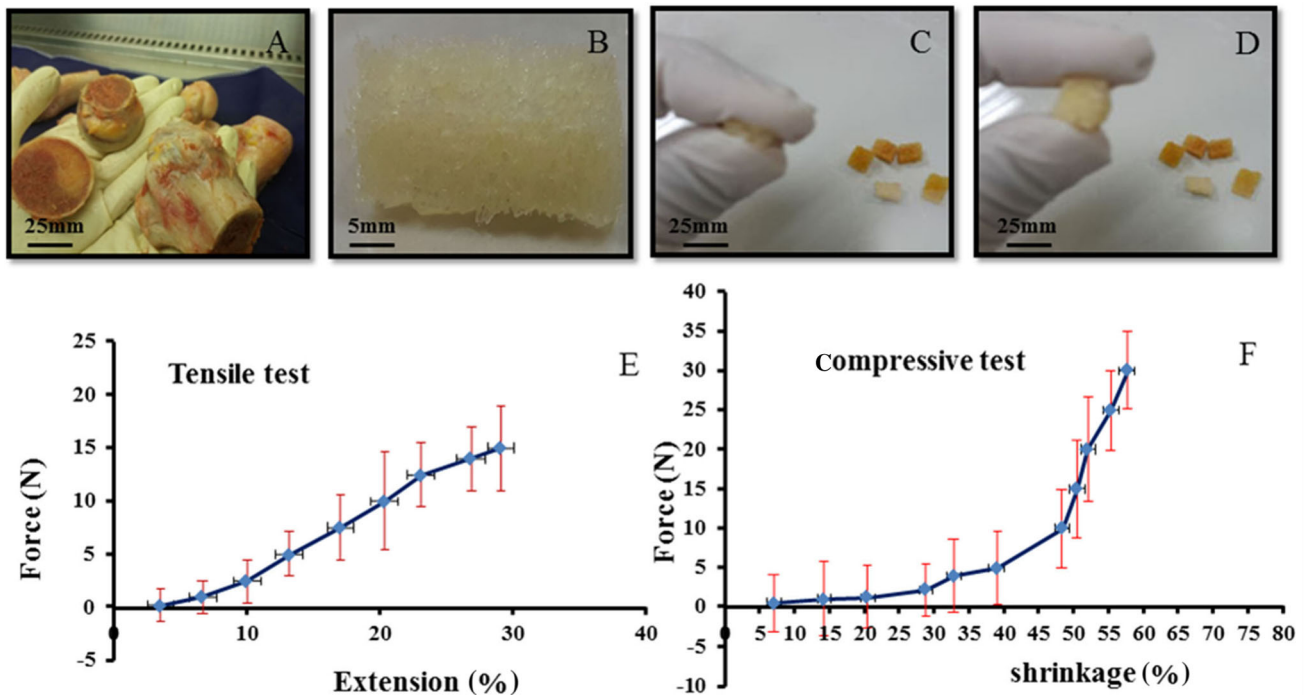


**Fig. 3** A Human bone as the raw material to produce DBM allograft scaffolds. B hDBM scaffolds. C, D Flexibility and compressibility of DBM allograft scaffolds. E Tensile test of allograft scaffolds.

**F** Compressive test of allograft scaffolds. The scaffolds have the potential of 57% elongation in the hydrated state

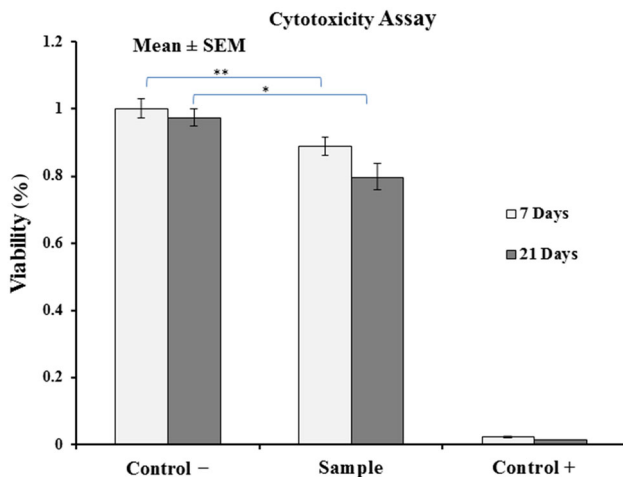


**Fig. 4** Viability of MSCs on scaffolds after 7 and 21 days (n = 3). Data are presented as mean ± standard error and indicate that the viability of cells is significant. The symbols (\*) and (\*\*) means ( $p < 0.05$ ) and ( $p < 0.01$ ), respectively

in the CHP + TGF group. Immunofluorescence evaluation revealed that the accumulation of type II collagen was much higher in CHP and CHP + TGF groups than the S + TGF group after three weeks, and the control group was not stained (Fig. 6C, D). This result supported the previous one (H&E staining), and there was a significant

difference between CHP, CHP + TGF, and S + TGF groups in this respect ( $p < 0.05$ ).

#### 4.7 Gene expression evaluation

Relative mRNA expression levels of Sox9, ACAN, Col1, Col2, osteocalcin, and RUNX2 were evaluated, which were normalized to GAPDH. Gene expression of Col1 in CHP, CHP + TGF, and S + TGF groups decreased after 21 days (Fig. 7), while it increased in S group. In addition, Col2 expression increased significantly in CHP and CHP + TGF groups, especially in CHP + TGF group. Sox9 and ACAN gene expression also increased in CHP and CHP + TGF groups. Comparison of CHP and CHP + TGF groups with the control (S group) showed significant differences ( $p < 0.05$ ). In addition, osteocalcin and RUNX2 genes were not significantly changed in CHP and CHP + TGF groups, while they were increased in S and S + TGF groups after 3 weeks.

#### 4.8 Glycosaminoglycan quantification

The differentiation stage of cells into chondrocyte can be determined by measurement of total GAG production in the culture medium [27, 28].

As shown in Fig. 8, GAG expression increased over time from days 7 to 21 in CHP + TGF and S + TGF

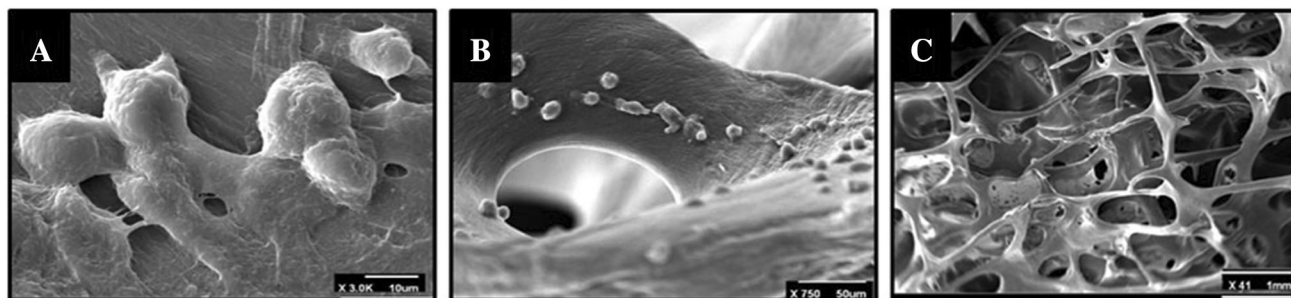


**Fig. 5** SEM image 48 h after cell seeding. **A** Cell morphology on scaffold with  $\times 3.0K$  magnification, **B** cell attachment on scaffold with  $\times 750$  magnification, **C** shows total structure of DBM scaffold with  $\times 41$  magnification

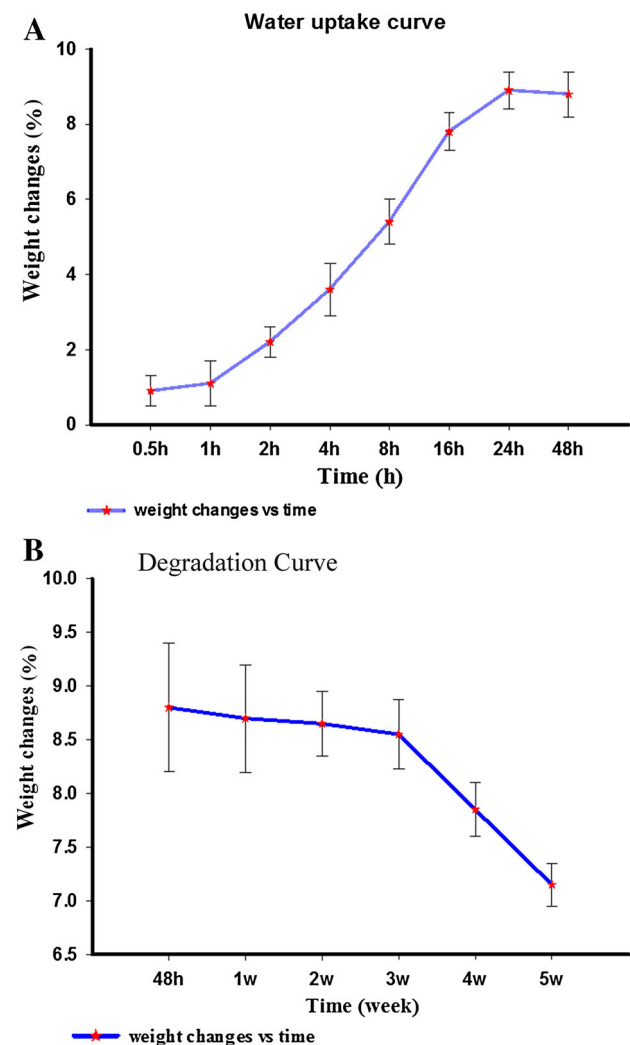


**Fig. 6** The scaffold weight changes in DW over time ( $n = 3$ ). Data are presented as mean  $\pm$  standard error. **A** Weight increase after 24 h due to water uptake; **B** Weight was decreased significantly after 3 weeks due to degradation

groups significantly ( $p < 0.05$ ). However, the expression levels of GAG in CHP samples significantly increased after loading in the end of third weeks ( $p < 0.001$ ). Furthermore,

in control group, there was no released GAG detected from days 7 to 21.

## 5 Discussion

Mechanical stimuli, type of scaffold being used, and type of cell in question are essentially the three factors influencing cartilage regeneration, as previously mentioned [9, 19]. Furthermore, it is widely believed that cell nutrition, proliferation, and migration are heavily affected by the porosity and pore size of the scaffolds [35]. Moreover, since mechanical properties of scaffolds can rapidly deteriorate due to a decrease in their structural density, these properties may actually be determined by the percentage of porosity. Also, it should be evaluated whether the samples have, in fact, both adequate mechanical and physical properties as the stimuli for cell growth. The physical results obtained in this study using DBM scaffolds confirmed that the samples provide sufficient porosity, permeability, interconnected pores of proper size (Fig. 2), and enough degradation time (Fig. 6). In this project, we hypothesized that the inherent flexibility of DBM scaffolds should trigger the application of a more efficient hydrostatic pressure to the cells, which consequently enhances cartilage differentiation. Moreover, taking into account the bone-like structure of these scaffolds and their inherent osteo-inductive properties, bone differentiation and formation can also be promoted at the same time in this approach [18, 36, 37]. Several studies have in fact indicated that at least one week of applying alternative hydrostatic pressure can lead to an increase in the expressions of Aggrecan and Col2 [28, 31, 36]. Gene expression results of our current study show that Col1 expression in CHP and CHP + TGF samples has been significantly reduced compared to the control sample (S) ( $p < 0.05$ ). In other words, hydrostatic pressure decreased differentiation to fibroblasts, while Col2 level significantly increased for both samples by nearly 1.4-fold ( $p < 0.05$ ). During skeletal development, Sox9 is a critical transcription factor in the



## Staining method

## Groups

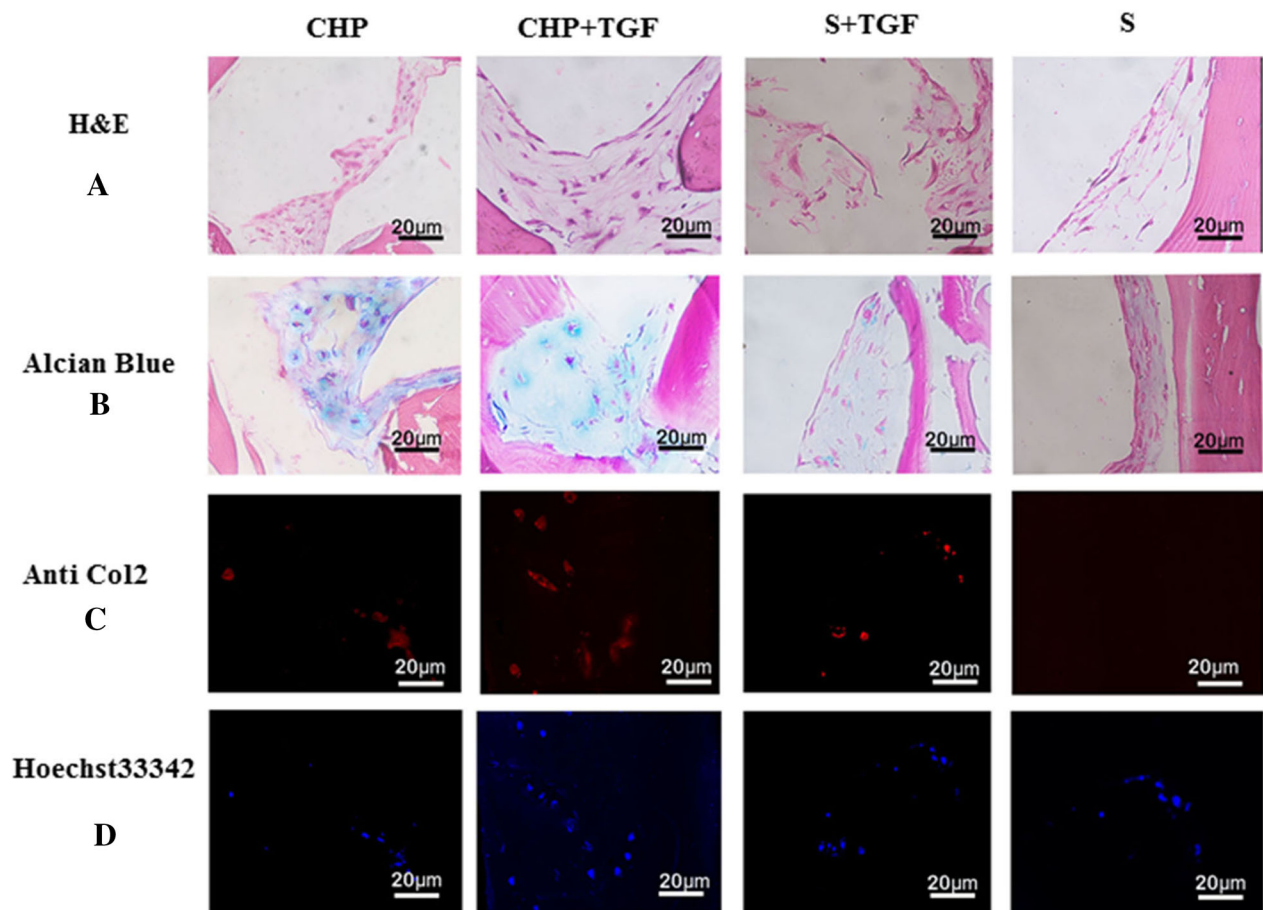


**Fig. 7** Histological staining of hBMSCs in different conditions and staining protocols. **A** H&E staining shows homogenous distribution of cells in the CHP and CHP + TGF and S + TGF groups with spherical to spindle-shaped cells. **B** Alcian blue staining shows a

positive reaction in both CHP and CHP + TGF groups. **C** Type II collagen immunofluorescence staining demonstrates positive reaction in the CHP and CHP + TGF and S + TGF groups, especially in the CHP + TGF group. **D** Hoechst staining shows cell nucleus

induction of a cartilage phenotype. In addition, for this particular transcription factor, type II collagen and ACAN (as the major proteins in a cartilage) contain binding sites in their promoters [38]. The data obtained from this study revealed that mRNA expression level of Sox9 was considerably increased for both CHP and CHP + TGF samples by 1.3- and 1.4-fold, respectively ( $p < 0.01$ ), while osteocalcin and RUNX2 levels were remarkably decreased in CHP and CHP + TGF samples as compared to the control sample ( $p < 0.05$ ). Furthermore, as mentioned earlier, ACAN level was increased in both samples by 1.7-

fold and 2.5-fold, respectively ( $p < 0.05$ ). The data also suggested that applying hydrostatic pressure on hBMSCs seeded in DBM scaffolds in the third weeks induced chondrogenic differentiation and inhibited osteogenic differentiation compared to the control sample (Fig. 9). Moreover, H&E staining method expressed that, in fact, all the cells changed into fusiform shape in the S group, while both fusiform and spherical cells were observed in CHP and CHP + TGF groups. The Alcian blue staining showed that the intracellular matrix in S group was not stained, while S + TGF and CHP groups were slightly stained, and

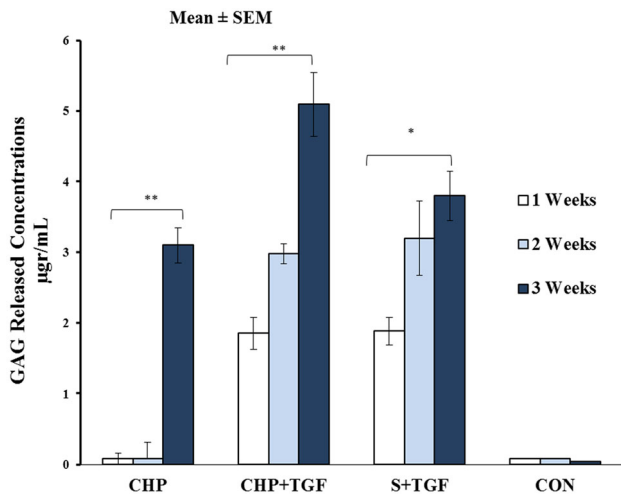


**Fig. 8** Comparison of total GAG release contents in different groups after 7, 14 and 21 days ( $n = 3$ ); the data are presented as Mean  $\pm$  standard error. (\*) indicates significant ( $p < 0.05$ ) and (\*\*) indicate very significant ( $p < 0.001$ )

considerable staining was observed in the case of CHP + TGF group. Based on this data, higher chondrogenic and lower osteogenic differentiation potential were observed in CHP and CHP + TGF samples. In addition, results

obtained from immunofluorescence staining were in good agreement with previous results achieved by H&E and Alcian blue staining methods. In other words, compared to the control group, CHP and CHP + TGF groups secreted Col2 and stained with Anti-Col2 (Fig. 7). Moreover, DMMB data determined that GAG secretion occurred in CHP, CHP + TGF, and S + TGF groups compared to the S group (Fig. 8), which was in good agreement with the other data obtained from real-time and histochemical staining.

In conclusion, DBM scaffolds have suitable properties such flexibility, interconnected porosity, enough degradation time and natural structural. Moreover Real-time and histochemical data collected in this study essentially show that chondrogenic and osteogenic differentiation can be achieved using a combination of these scaffolds with hydrostatic pressure. Therefore, hydrostatic loading decreases osteogenic properties in favor of chondrogenic ones. Since the cells in articular cartilage are under hydrostatic pursue, this study can be a basic step in the application of DBM in cartilage regeneration. Consequently, it is possible to develop a novel scaffold that supports the bone from one side and helps regenerate the cartilage from the other side.

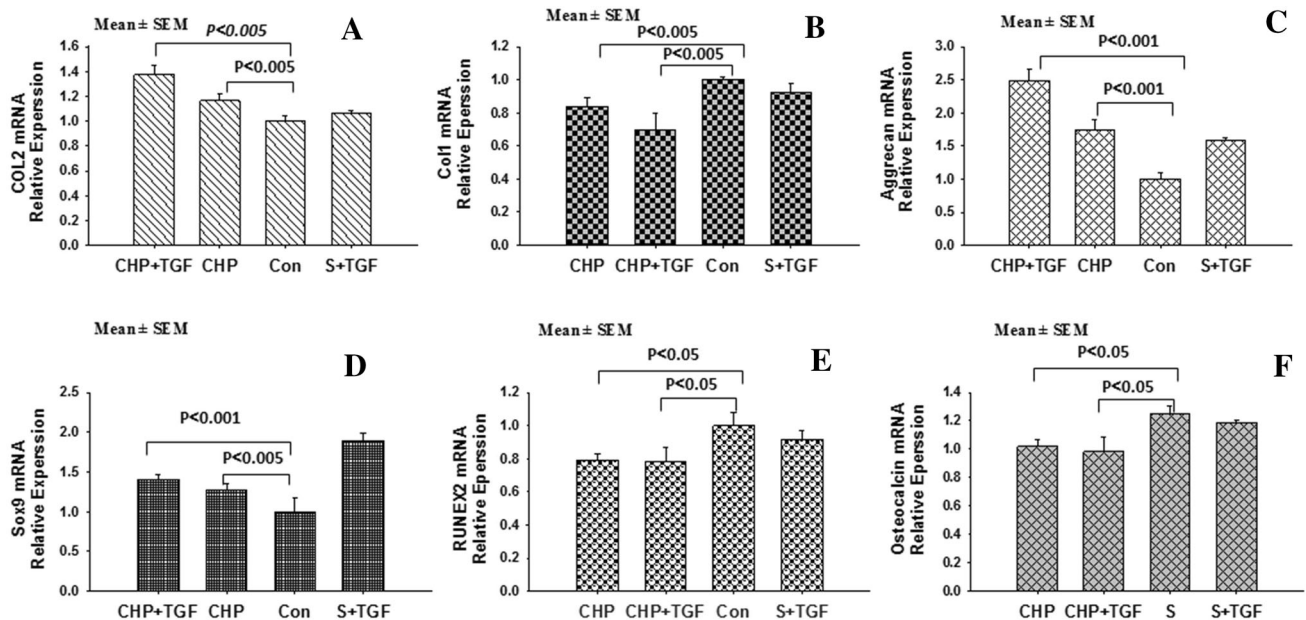


**Fig. 9** The mRNA expression level of different genes in different groups. The data were normalized to GAPDH value; the data are presented as mean  $\pm$  standard error ( $n = 3$ ). Values of  $p < 0.05$  were considered as significant. **A** Type II collagen mRNA expression increased in samples CHP and CHP + TGF. **B** Type I collagen

mRNA expression level decreased in CHP and CHP + TGF. **C**, **D** Indicate Sox9 and ACAN mRNA expression level increased in CHP and CHP + TGF samples, significantly. **E**, **F** Show RUNEX2 and Osteocalcin mRNA expression level decreased in mentioned samples, significantly

**Acknowledgements** The authors would like to express their appreciation to Alborz Balk Pharmaceutical Company, Nano Zist Arrayeh, and Dr. Kayvan pathology lab for their generous support. This study was supported by Iran Pasteur Institute research (Grant No. 861).

#### Compliance with ethical standards

**Conflict of interest** The authors declare that they have no conflict of interest.

**Ethical statement** There are no animal experiments carried out in this article. However, tissue removal from donors was carried out according to Iran Brain death law and Iran Tissue Bank Standards. Ethical and technical proses had been approved by Iran Food and Drug Administration (664/188547).

#### References

- Mobasheri A, Csaki C, Clutterbuck AL, Rahmanzadeh M, Shakibaei M. Mesenchymal stem cells in connective tissue engineering and regenerative medicine: applications in cartilage repair and osteoarthritis therapy. *Histol Histopathol*. 2009;24:347–66.
- Redman SN, Oldfield SF, Archer CW. Current strategies for articular cartilage repair. *Eur Cell Mater*. 2005;9:23–32.
- Werkmeister JA, Adhikari R, White JF, Tebb TA, Le TP, Taing HC, et al. Biodegradable and injectable cure-on-demand polyurethane scaffolds for regeneration of articular cartilage. *Acta Biomater*. 2010;6:3471–81.
- Hwang NS, Varghese S, Elisseeff J. Cartilage tissue engineering: directed differentiation of embryonic stem cells in three-dimensional hydrogel culture. *Methods Mol Biol*. 2007;407:351–73.
- Getgood A, Brooks R, Fortier L, Rushton N. Articular cartilage tissue engineering: today's research, tomorrow's practice? *J Bone Joint Surg Br*. 2009;91:565–76.
- Shao XX, Huttmacher DW, Ho ST, Goh JC, Lee EH. Evaluation of a hybrid scaffold/cell construct in repair of high-load-bearing osteochondral defects in rabbits. *Biomaterials*. 2006;27:1071–80.
- Lutolf MP, Hubbell JA. Synthetic biomaterials as instructive extracellular microenvironments for morphogenesis in tissue engineering. *Nat Biotechnol*. 2005;23:47–55.
- Zheng L, Fan HS, Sun J, Chen XN, Wang G, Zhang L, et al. Chondrogenic differentiation of mesenchymal stem cells induced by collagen-based hydrogel: an in vivo study. *J Biomed Mater Res A*. 2010;93:783–92.
- Zheng L, Yang J, Fan H, Zhang X. Material-induced chondrogenic differentiation of mesenchymal stem cells is material-dependent. *Exp Ther Med*. 2014;7:1147–50.
- Bonakdar S, Emami SH, Shokrgozar MA, Farhadi A, Ahmadi SAH, Amanzadeh A. Preparation and characterization of polyvinyl alcohol hydrogels crosslinked by biodegradable polyurethane for tissue engineering of cartilage. *Mater Sci Eng C Mater Biol Appl*. 2010;30:636–43.
- Derakhshan ZH, Shaghagh B, Asl MP, Majidi M, Ghazizadeh L, Chegini A, et al. In situ forming hydrogel based on chondroitin sulfate–hydroxyapatite for bone tissue engineering. *Int J Polym Mater*. 2015;64:919–26.
- Karkhaneh A, Naghizadeh Z, Shokrgozar MA, Bonakdar S. Evaluation of the chondrogenic differentiation of mesenchymal stem cells on hybrid biomimetic scaffolds. *J Appl Polym Sci*. 2014;131:40635.
- Shokrgozar MA, Bonakdar S, Dehghan MM, Emami SH, Montazeri L, Azari S, et al. Biological evaluation of polyvinyl alcohol hydrogel crosslinked by polyurethane chain for cartilage tissue engineering in rabbit model. *J Mater Sci Mater Med*. 2013;24:2449–60.
- Downes S, Archer RS, Kayser MV, Patel MP, Braden M. The regeneration of articular cartilage using a new polymer system. *J Mater Sci Mater Med*. 1994;5:88–95.
- Bauer TW, Muschler GF. Bone graft materials: an overview of the basic science. *Clin Orthop Relat Res*. 2000;371:10–27.
- Harakas NK. Demineralized bone-matrix-induced osteogenesis. *Clin Orthop Relat Res*. 1984;188:239–51.
- Chakkalakal DA, Strates BS, Garvin KL, Novak JR, Fritz ED, Mollner TJ, et al. Demineralized bone matrix as a biological scaffold for bone repair. *Tissue Eng*. 2001;7:161–77.
- Gruskin E, Doll BA, Futrell FW, Schmitz JP, Hollinger JO. Demineralized bone matrix in bone repair: history and use. *Adv Drug Deliv Rev*. 2012;64:1063–77.
- Kelly DJ, Jacobs CR. The role of mechanical signals in regulating chondrogenesis and osteogenesis of mesenchymal stem cells. *Birth Defects Res C Embryo Today*. 2010;90:75–85.
- Choi JR, Yong KW, Choi JY. Effects of mechanical loading on human mesenchymal stem cells for cartilage tissue engineering. *J Cell Physiol*. 2018;233:1913–28.
- Fahy N, Alini M, Stoddart MJ. Mechanical stimulation of mesenchymal stem cells: implications for cartilage tissue engineering. *J Orthop Res*. 2018;36:52–63.
- Thorpe S, Buckley C, Vinardell T, O'Brien FJ, Campbell V, Kelly DJ. Dynamic compression can inhibit chondrogenesis of mesenchymal stem cells. *Biochem Biophys Res Commun*. 2008;377:458–62.
- Thorpe S, Buckley C, Vinardell T, O'Brien FJ, Campbell V, Kelly DJ. The response of bone marrow-derived mesenchymal stem cells to dynamic compression following TGF- $\beta$ 3 induced chondrogenic differentiation. *Ann Biomed Eng*. 2010;38:2896–909.
- Huang AH, Farrell MJ, Kim M, Mauck RL. Long-term dynamic loading improves the mechanical properties of chondrogenic mesenchymal stem cell-laden hydrogels. *Eur Cells Mater*. 2010;19:72–85.
- Angele P, Yoo JU, Smith C, Mansour J, Jepsen KJ, Nerlich M, et al. Cyclic hydrostatic pressure enhances the chondrogenic phenotype of human mesenchymal progenitor cells differentiated in vitro. *J Orthop Res*. 2003;21:451–7.
- Miyamishi K, Trindade MC, Lindsey DP, Beaupré GS, Carter DR, Goodman SB, et al. Effects of hydrostatic pressure and transforming growth factor- $\beta$ 3 on adult human mesenchymal stem cell chondrogenesis in vitro. *Tissue Eng*. 2006;12:1419–28.
- Wagner DR, Lindsey DP, Li KW, Tummala P, Chandran SE, Smith RL, et al. Hydrostatic pressure enhances chondrogenic differentiation of human bone marrow stromal cells in osteochondrogenic medium. *Ann Biomed Eng*. 2008;36:813–20.
- Ogawa R, Mizuno S, Murphy GF, Orgill DP. The effect of hydrostatic pressure on three-dimensional chondroinduction of human adipose-derived stem cells. *Tissue Eng Part A*. 2009;15:2937–45.
- Meyer EG, Buckley CT, Steward AJ, Kelly DJ. The effect of cyclic hydrostatic pressure on the functional development of cartilaginous tissues engineered using bone marrow derived mesenchymal stem cells. *J Mech Behav Biomed Mater*. 2011;4:1257–65.
- Karkhaneh A, Naghizadeh Z, Shokrgozar MA, Bonakdar S, Solouk A, Haghhighipour N. Effects of hydrostatic pressure on biosynthetic activity during chondrogenic differentiation of MSCs in hybrid scaffolds. *Int J Artif Organs*. 2014;37:142–8.
- Puetzer J, Williams J, Gillies A, Bernacki S, Lobo EG. The effects of cyclic hydrostatic pressure on chondrogenesis and viability of human adipose- and bone marrow-derived

- mesenchymal stem cells in three-dimensional agarose constructs. *Tissue Eng Part A*. 2012;19:299–306.
32. Wagers AJ, Sherwood RI, Christensen JL, Weissman IL. Little evidence for developmental plasticity of adult hematopoietic stem cells. *Science*. 2002;297:2256–9.
  33. Prockop DJ. Marrow stromal cells as stem cells for non-hematopoietic tissues. *Science*. 1997;276:71–4.
  34. Bruder SP, Fink DJ, Caplan AI. Mesenchymal stem cells in bone development, bone repair, and skeletal regeneration therapy. *J Cell Biochem*. 1994;56:283–94.
  35. Lien SM, Ko LY, Huang TJ. Effect of pore size on ECM secretion and cell growth in gelatin scaffold for articular cartilage tissue engineering. *Acta Biomater*. 2009;5:670–9.
  36. Hall AC, Urban JP, Gohl KA. The effects of hydrostatic pressure on matrix synthesis in articular cartilage. *J Orthop Res*. 1991;9:1–10.
  37. Zimmermann G, Moghaddam A. Allograft bone matrix versus synthetic bone graft substitutes. *Injury*. 2011;42:S16–21.
  38. Cao L, Yang F, Liu G, Yu D, Li H, Fan Q et al. The promotion of cartilage defect repair using adenovirus mediated Sox9 gene transfer of rabbit bone marrow mesenchymal stem cells. *Bio-materials*. 2011;32:3910–20.